J Radioanal Nucl Chem (2015) 306:283–288
DOI 10.1007/s10967-015-4175-5

# Characterization of uranium and thorium containing minerals by nuclear microscopy

**Zsófia Kertész[1] · Enikő Furu[1] · Anikó Angyal[1] · Ágnes Freiler[2,3] · Kálmán Török[3] · Ákos Horváth[2]**

Received: 11 July 2014 / Published online: 26 May 2015


**Abstract** Radioactive minerals of the gneiss of Sopron Mountains were analysed by micro-PIXE method at the Debrecen scanning nuclear microprobe. Zircon and monazite minerals were identified with detectable amount of U and Th. Qualitative elemental maps and quantitative concentration data were obtained on 20 minerals. U and Th concentrations were between few 100 ppm and 10 wt%. The size of the minerals varied between few micrometers and 100 microns, the distribution of U and Th within the grains was inhomogeneous. These radioactive minerals occurred in veins enriched with Fe.

**Keywords** Nuclear microscopy · Scanning nuclear microprobe · Micro-PIXE · Sopron hills · Gneiss · Radioactive minerals

## Introduction

The main rock types of Sopron mountains are gneiss and micaschist formed from granite and sedimentary rocks at about 1,3–1,4 GPa pressure and about 550–580 °C temperature during the Alpine metamorphism [1, 2]. There are several retrograde metamorphic and near-surface processes that happened after the peak of the metamorphism, like plastic deformation, phosphate mineralization and argillitic limonitic alteration in certain zones. These processes involved fluid migration and fluid-rock interactions and locally may have increased the U, Ra and Th activity concentration in the rocks of the Sopron Mts [3, 4]. Deformed gneisses were described in several places in the Sopron Mountains. One of the localities is the Csalóka Spring, where both the water and the deformed gneiss samples show anomalously high radon and radium activity compared with most of the gneisses in the Sopron Mountains [5, 6]. In this paper we present mineralogical evidence of the presence and enrichment of U and Th bearing minerals of the deformed gneiss samples around the Csalóka Spring, Sopron Mountains. We used petrographical microscope and scanning electron microscope (SEM) to detect the Th and U-bearing minerals and to define their textural position and origin in the deformed gneiss samples. Besides, micro-PIXE was used to determine the composition of these radioactive minerals as well as their chemical/mineralogical environment, and local activity concentration. The gathered data on the distribution of U and Th bearing minerals and their chemical composition can help us to describe and characterize the geological processes leading to these radioactive anomalies.

Particle induced X-ray emission analysis (PIXE) performed on the Debrecen nuclear microprobe was used to provide quantitative information about the major and trace element content of the samples on a micrometer scale. Ion beam analytical methods, including micro-PIXE has many advantages in the characterization of mineral samples with complex structures, as it was demonstrated in these studies [7–11]. The 2–3 MeV $H^+$ beam penetrates few tens of micrometers into the sample with negligible spread and without sample destruction. The method is fully quantitative, and

✉ Zsófia Kertész
kertesz.zsofia@atomki.mta.hu

[1] Laboratory of Ion Beam Applications, Institute for Nuclear Research, Hungarian Academy of Sciences, Bem tér 18/c, Debrecen 4026, Hungary

[2] Department of Atomic Physics, Eötvös Loránd University, Pázmány Péter stny. 1/A, Budapest 1117, Hungary

[3] Geological and Geophysical Institute of Hungary, Stefánia út 14, Budapest 1143, Hungary

most cases the use of standards is not required. The detection limits are low (1–20 ppm), thus trace elements can be determined and mapped. The high resolution 2D imaging provides textural information. The above listed features make nuclear microscopy an ideal complementary technique to electron probe microanalysis.

## Materials and methods

Polished thin sections of deformed gneiss collected at the Csalóka Spring were selected to conduct petrographic microscopic and scanning electron microscopic (SEM) study to describe the minerals and the texture of the rocks. Autoradiography, using solid state nuclear track detectors were also carried out on the samples. As a next step the most interesting areas were studied by ion microscopy at the scanning nuclear microprobe installed on the 0° beamline of the 5 MV Van de Graaff accelerator of Atomki [12]. A proton beam of 2 MeV energy focused down to 2 μm × 2 μm with a current of 300–500 pA was used to irradiate the samples. Two Si (Li) X-ray detectors placed at 135° geometry to the incidence beam were applied to collect the emitted characteristic X-rays. A detector with ultra-thin polymer window (UTW) was used to measure low- and medium-energy X-rays ($Z > 5$), and a Be windowed detector equipped with an additional Kapton filter of 250 μm thickness was applied to detect the medium and high energy X-rays ($Z > 20$). The beam dose was measured with a beam chopper. This way all composing elements could be measured in the same time, reducing both measurement time and sample damage. Signals from all detectors were recorded event by event in list mode by the Oxford type OMDAQ data acquisition system [13]. More detailed description of the measurement setup and data acquisition system can be found in [14–16].

At first elemental maps of a 1 mm × 1 mm area were recorded to find the possible U and Th containing minerals. Usually U and Th replace rare earth elements in different minerals, therefore we looked for Zr, Ce, La and Y since these elements occur in higher concentration and have less overlapping peaks. Once the potentially interesting areas were identified the scan size was reduced, and the U and Th containing minerals were studied in more details. Quantitative measurements were done either in masked areas or in points. The data acquisition system makes it possible to subtract the required information off-line, if needed.

Spectra of a monazite recorded with the two detectors are presented in Fig. 1a, b. The obtained PIXE spectra were evaluated with the GUPIXWIN program code [17]. At first the composition of the matrix was determined from the spectra of the UTW detector using the iterative matrix solution method, and then the spectra of the Be windowed

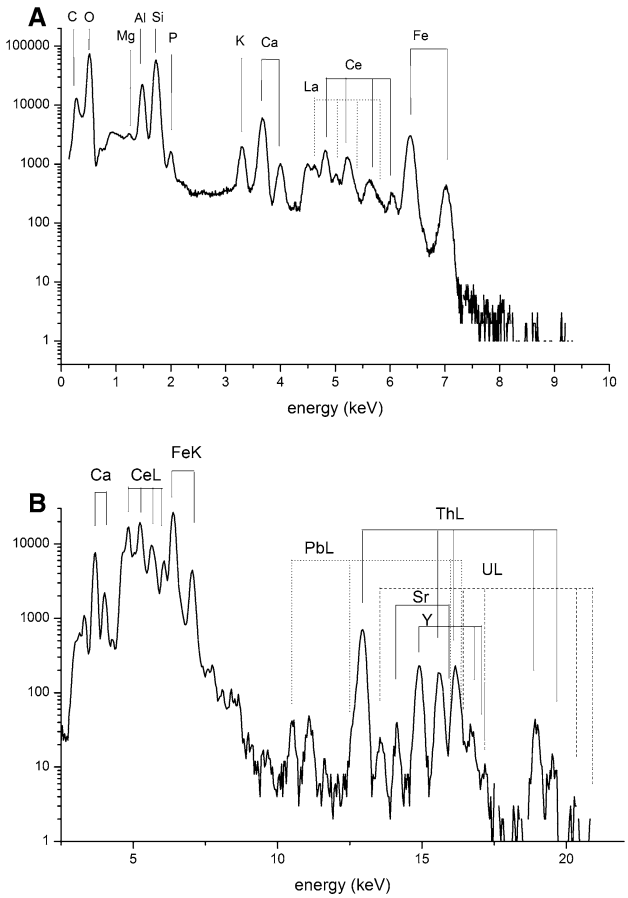


**Fig. 1** **a** Micro-PIXE spectra recorded on a monazite spot with the UTW detector. The presence of carbon is due to the C layer used for SEM. It was not removed completely to give a conductive layer avoiding sample charging effect. In GUPIXWIN it was handled as surface element. **b** Micro-PIXE spectra recorded on a monazite spot with the Be windowed detector

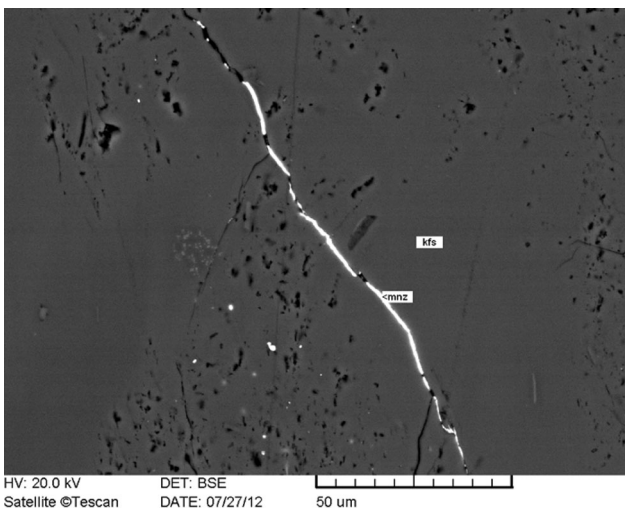


**Fig. 2** Backscattered electron image of K-feldspar (kfs) crosscut by thin discontinuous monazite (mnz) veinlet

detector was analysed in trace element mode, using the previously obtained matrix. On the spectra of both detectors the X-ray energy range of 3.0–8.5 keV is common, therefore intensive X-ray lines within this range (e.g. Ca Kα, Fe Kα, Ce Lα), was used to normalize the elemental concentrations. In most cases the differences of the concentration values of the two detector were 0–5 %. As a final step, the elemental composition was normalized to 100 %, if needed.

## Results and discussion

We studied a selected deformed gneiss sample under the petrographic microscope and SEM to see the minerals and texture of the sample. The deformed gneiss consists mainly of quartz, albite, K-feldspar, muscovite with minor amounts of biotite, garnet and accessory apatite, monazite, zircon, rutile and ilmenite. Deformation of the gneiss caused that planar features and mylonitic zones appeared in the previously unoriented rocks. Undulatory extinction, subgrain formation, development of mortar texture in quartz, and feldspars and kinking and preferred orientation of micas as features of deformation are clearly observable in the rock under the microscope. The mylonitic zones as well as the mica rich layers with preferred orientation may serve as the primary places of fluid migration. U and Th-bearing minerals in the gneisses are relatively rare, however, in the deformed gneiss they are sometimes enriched in mylonitic zones and in mica-rich layers. Scanning electron microscopic studies revealed the presence of several U and Th bearing minerals like: zircon ($ZrSiO_4$) (U), monazite ($CePO_4$) (U; Th), cheralite ($CaTh(PO4)_2$) (Th), allanite (U; Th), $[(Ce,Ca,Y,La)_2(Al,Fe^{+3})_3(-SiO4)_3(OH)]$, xenotime ($YPO_4$) (U; Th) and an undeterminable U-oxide phase. The secondary nature of most of

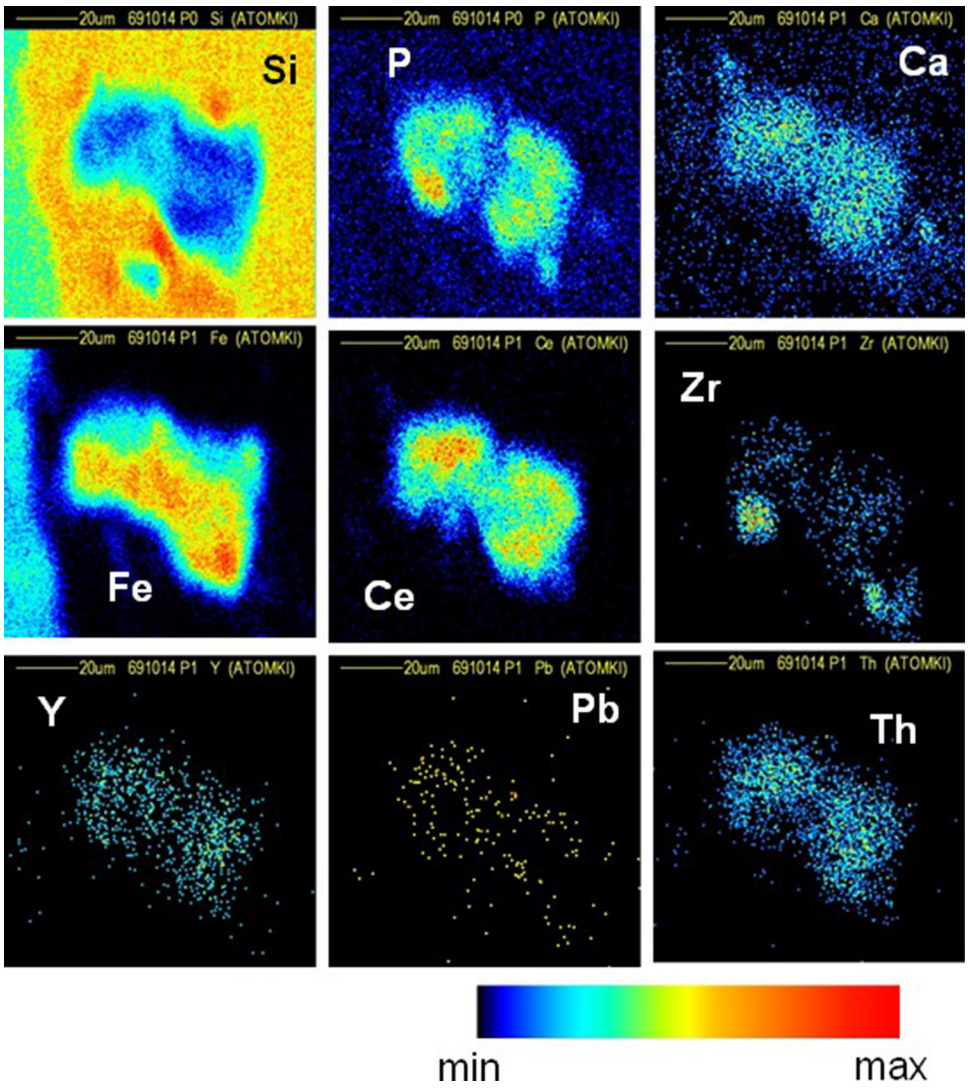


**Fig. 3** Elemental maps recorded on a monazite inclusion in the DU2CS1 sample at the Debrecen scanning nuclear microprobe. Scan size was 100 × 100 μm

these minerals are evident, as they occur along certain zones, in the interstices or in cracs (Fig. 2), while the original U and Th-bearing minerals of the gneisses tend to occur as inclusions in the rock forming minerals. The mineralized zones are also enriched in Ti–Fe oxides and Fe-oxide-hydroxides. A unique very thin veinlet of monazite in a fracture crosscutting K-feldspar was also observed (Fig. 2) as a good evidence of the secondary nature of enrichment of the U and Th-bearing minerals.

The rock forming minerals (quartz, muscovite, albite, K-feldspar, biotite, garnet, apatite) of the samples did not contain detectable amount of U and Th (DL was ~50 ppm). However, monazite and zircon minerals were found in the samples which had varying U and Th content. The size of these minerals varied from few micrometres to 100 microns. They could occur together and separate, too. Qualitative elemental maps of a monazite grain with attached zircon in the DU2CS1 sample (Csalóka Spring) are shown on Fig. 3.

Within this mineral four spots were analysed. PIXE spectra of one monazite was shown on Fig. 1a, b. Spectra of a zircon mineral are shown on Fig. 4a, b. For mapping purposes such X-ray lines of a given element were chosen with which no other element has overlapping peaks. Therefore for example in the case of Th mapping the Th $L_{\alpha 1}$ and for mapping of U the U $L_{\beta 1}$ and U $L_{\gamma}$ lines were used.

The results of this quantitative analysis are summarized in Table 1. It indicates that the monazite is Ce-rich with 5–7 % Th content. U and Pb content ranged from 2000 to 4000, and from 1000 to 1500 ppm, respectively. Y was present at 1–1.5 wt%.

In the case of zircon the Th content was ~1 wt%, and U occurred in 1300–1800 ppm. It contained Hf and Y in few thousand ppm concentration.

It can be seen from the maps and also from the quantitative concentration data that the distribution of Th and Pb as well as U is inhomogeneous within the grains. Monazite occurred together with Fe while zircon grains situated next to iron-bearing veins. If we consider the large amounts of monazite analyses made in the metamorphic rocks of the Sopron Mountains it seems that the iron, especially in large quantities, is not part of the monazite or zircon chemistry [4]. Thus we assume that the presence of iron may be attributed to iron oxides-hydroxide minerals coating the original monazite or zircon grains. The chemical incompatibility of iron with monazite suggested by literature measurements [4] and the relatively homogeneous distribution of iron, cerium and phosphorus (Fig. 2) indicates that the apparently large iron-bearing monazite is rather a very fine grained aggregate of monazite and iron-oxide-hydroxides. These iron-oxides-hydroxides are observable during the microscopic study of the thin sections as brownish colorations in the deformed zones.

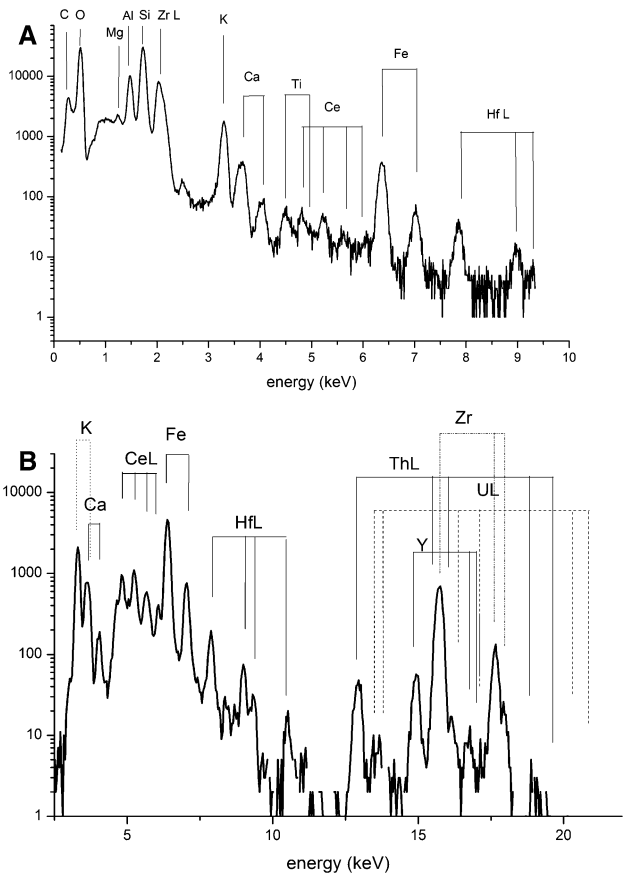


**Fig. 4** **a** Micro-PIXE spectra recorded on a zircon spot with the UTW detector. **b** Micro-PIXE spectra recorded on a masked area on zircon with the Be windowed detector

The simultaneous determination of Pb, Th and U allows the determination of geological ages corresponding to the mineral (monazite, zircon) formation [11, 18, 19]. Assuming that the amount of common Pb and Pb diffusion is negligible the measured Pb concentration can be derived only by Th and U decay. In this presented example Pb was found under detection limit in the zircon spots, which means that the age of these minerals were younger than 80–100 M years. In the case of the monazite the mineral could be dated at 400 ± 40 Ma using the method described in [19]. However, as we mentioned in the previous paragraph, the structure of the mineral and the presence of other, non-monazite-composing elements indicates, that this monazite is a fine aggregate rather than a single crystal. This means that the presence of natural lead cannot be excluded, therefore this dating method cannot be applied in this case.

According to this finding, in the future we plan to carry out systematic and precise point measurements on the samples in order to achieve reliable geological ages.

**Table 1** Elemental concentrations, fit error and detection limits in four selected spots on DU2CS1 sample

| | Monazite 1 | | Monazite 2 | | | Zircon 1 | | Zircon 2 | | |
|---|---|---|---|---|---|---|---|---|---|---|
| | Conc. (ppm) | Error (%) | Conc. (ppm) | Error (%) | DL (ppm) | Conc. (ppm) | Error (%) | Conc. (ppm) | Error (%) | DL (ppm) |
| O | 361,700 | 1 | 340,600 | 1 | 383 | 384,800 | 1 | 427,100 | 1 | 409 |
| Na | 4735 | 10 | | | 741 | 24,400 | 28 | 17,200 | 4 | 967 |
| Mg | 1435 | 21 | 1815 | 25 | 517 | 800 | 57 | 2650 | 17 | 643 |
| Al | 64,500 | 1 | 29,400 | 2 | 430 | 43,200 | 1 | 80,650 | 1 | 526 |
| Si | 142,000 | 1 | 89,700 | 1 | 342 | 203,800 | 1 | 237,300 | 1 | 431 |
| P | 74,900 | 1 | 94,300 | 1 | 285 | 28,800 | 5 | 12,500 | 7 | 2297 |
| S | 890 | 23 | 390 | 86 | 302 | | | | | |
| Cl | 600 | 24 | 330 | 67 | 252 | 630 | 29 | | | 250 |
| K | 7000 | 3 | 2370 | 12 | 290 | 51,600 | 1 | 17,600 | 2 | 220 |
| Ca | 30,900 | 1 | 38,000 | 1 | 241 | 9700 | 4 | 15,270 | 2 | 234 |
| Sc | 430 | 35 | | | 300 | 515 | 25 | 350 | 25 | 90 |
| Ti | 410 | 29 | 1160 | 14 | 279 | 315 | 29 | 240 | 28 | 72 |
| Fe | 52,300 | 2 | 97,400 | 1 | 222 | 26,800 | 2 | 19,200 | 2 | 59 |
| Zn | 120 | 26 | | | 56 | | | | | |
| Sr | 1300 | 11 | 920 | 29 | 93 | 230 | 75 | 175 | 75 | 105 |
| Y | 10,700 | 4 | 14,900 | 5 | 350 | 8720 | 8 | 6680 | 8 | 312 |
| Zr | 1000 | 34 | | | 1057 | 161,400 | 2 | 123,300 | 2 | 950 |
| La | 44,300 | 3 | 54,100 | 3 | 875 | 8350 | 8 | 5900 | 8 | 245 |
| Ce | 95,000 | 2 | 105,600 | 2 | 614 | 17,300 | 4 | 12,600 | 4 | 219 |
| Nd | 41,300 | 3 | 46,600 | 3 | 2771 | 8,600 | 5 | 6200 | 5 | 519 |
| Sm | 7150 | 8 | 6950 | 16 | 2162 | 1200 | 30 | 890 | 29 | 448 |
| Pb | 1150 | 12 | 1375 | 18 | 149 | 470 | 44 | 375 | 44 | 144 |
| Bi | 230 | 59 | | | 157 | 5200 | 5 | 4070 | 5 | 159 |
| Th | 53,400 | 2 | 70,600 | 3 | 430 | 11,420 | 9 | 8740 | 9 | 370 |
| U | 1930 | 17 | 3600 | 19 | 202 | 1750 | 36 | 1330 | 36 | 262 |

## Summary

In this work all together three samples, 12 1 mm × 1 mm scans were studied using micro-PIXE method at the Debrecen scanning nuclear microprobe. Quantitative analysis has been done on 20 minerals. U and Th containing minerals such as monazite and zircon were identified. The U and Th content of the monazite and zircon varied between few hundred ppm and 10 wt%. In general, zircon contained U and monazite Th in higher concentrations. Although some bigger grains were also found, most of the U and Th containing minerals were small with dimensions between 2 and 20 μm. We showed that the radioactive minerals occurred in veins, sometimes enriched in Fe. This finding indicates that the increase of U and Th in the Fe rich veins was caused by precipitation of monazite, zircon and other U and Th-bearing minerals during deformation of the gneiss as a result of retrograde fluid-rock interaction. The literature data, the complex chemistry and the distribution of main and trace elements in the studied minerals indicates that these minerals represent an aggregate of monazite, zircon and iron oxides-hydroxides rather than pure mineral grains. The quite homogeneous distribution of iron shows that the individual grains of the mineral aggregate are smaller than the spatial resolution of the PIXE.

We also demonstrated that nuclear microscopy, due to its high spatial resolution and the low detection limits proved to be a powerful tool for the characterization of minerals with complex chemistry and it serves as an ideal complementary technique of optical mineralogy and SEM.

**Acknowledgments** This research was supported by the European Union and the State of Hungary, co-financed by the European Social Fund in the framework of TÁMOP 4.2.4.A/2-11-1-2012-0001 'National Excellence Program'. This paper was supported by the János Bolyai Research Scholarship of the Hungarian Academy of Sciences.

## References


1. Török K (1998) Magmatic and high pressure metamorphic development of orthogneisses in the Sopron area, Eastern Alps (W-Hungary). N Jahrb Mineral Abh 173:63–91
2. Török K (2003) Alpine P-T path of micaschists and related orthogneiss veins near Óbrennberg (W-Hungary, Eastern Alps). Neues Jahrb Mineral Abh 179(2):101–142
3. Török K (2001) Multiple fluid migration events in the Sopron Gneisses during the Alpine high-pressure metamorphism, as recorded by bulk-rock and mineral chemistry and fluid inclusions. Neues Jahrb Mineral Abh J Mineral Geochem 177(1): 1–36
4. Nagy G, Draganits E, Demény A, Gy Pantó, Árkai P (2002) Genesis and transformations of monazite, florencite and rhadophane during medium grade metamorphism: examples from the Sopron Hills Eastern Alps. Chem Geol 191:25–46
5. Freiler Á, Horváth Á, Török K, Földes T, Origin of radon concentration of Csalóka Spring, Sopron Hills, West Hungary (will be submitted later)
6. Freiler Á, Horváth Á, Török K (2015) $^{226}$Ra activity distribution of rocks in the Sopron Mts. (West Hungary). J Radioanal Nucl Chem. doi:10.1007/s10967-014-3914-3
7. Wilson GC, Rucklidge JC, Campbell JL, Nejedly Z, Teesdale WJ (2002) Application of PIXE to mineral characterization. Nucl Instr Phys Res B 189:387–393
8. Ryan CG, van Achterberg E, Yeats CJ, Win TT, Cripps G (2002) Quantitative PIXE trace element imaging of minerals using the new CSIRO-GEMOC nuclear microprobe. Nucl Instr Phys Res B 189:400–407
9. Vaggelli G, Borghi A, Cossio R, Fedi M, Giuntini L, Lombardo B, Marino A, Massi M, Olmi F, Petrelli M (2006) Micro-PIXE analysis of monazite from the Dora Maira Massif, Western Italian Alps. Microchim Acta 155:305–311
10. Ohnuki T, Kozai N, Samadfan M, Yasuda R, Yasuda R, Kamiya T, Sakai T, Murakami T (2001) Analysis of uranium distribution in rocks by μ-PIXE. Nucl Instr Phys Res B 181:586–592
11. Lekki J, Lebed S, Paszkowski ML, Kusiak M, Vogt J, Hajduk R, Polak W, Potempa A, Stachura Z, Styczen J (2003) Age determination of monazite using the new experimental chamber of the Cracow proton microprobe. Nucl Instr Phys Res B 210:472–477
12. Rajta I, Borbély-Kiss I, Mórik Gy, Bartha L, Koltay E, Kiss ÁZ (1996) The new ATOMKI scanning proton microprobe. Nucl Instr Methods B 109–110:148–153
13. Grime GW, Dawson M (1995) Recent developments in data acquisition and processing on the Oxford scanning proton microprobe. Nucl Inst Methods B 104:107
14. Uzonyi I, Rajta I, Bartha L, Kiss ÁZ, Nagy A (2001) Realization of the simultaneous micro-PIXE analysis of heavy and light elements at a nuclear microprobe. Nucl Instr Methods B 181(1–4):193–198
15. Zs Kertész, Szikszai Z, Szoboszlai Z, Simon A, Huszánk R, Uzonyi I (2009) Study of individual atmospheric aerosol particles at the Debrecen ion microprobe. Nucl Instr Methods B 267:2236–2240
16. Zs Kertész, Szikszai Z, Uzonyi I, Simon A, Kiss ÁZ (2005) Development of a bio-PIXE setup at the Debrecen scanning proton microprobe. Nucl Instr Methods B 231:106–111
17. Campbell JL, Boyd NI, Grassi N, Bonnick P, Maxwell JA (2010) The Guelph PIXE software package IV. Nucl Instr Methods B268(2010):3356–3363
18. Mazzoli C, Hanchar JM, Della Mea G, Donovan JJ, Stern RA (2002) μ-PIXE analysis of monazite for total U-Th-Pb age determination. Nucl Instr Methods B 189:394–395
19. Montel JM, Foret S, Veschambre M, Nicollet C, Provost A (1996) Electron microprobe dating of monazite. Chem Geol 131:37–53